ChemComm

Accepted Manuscript

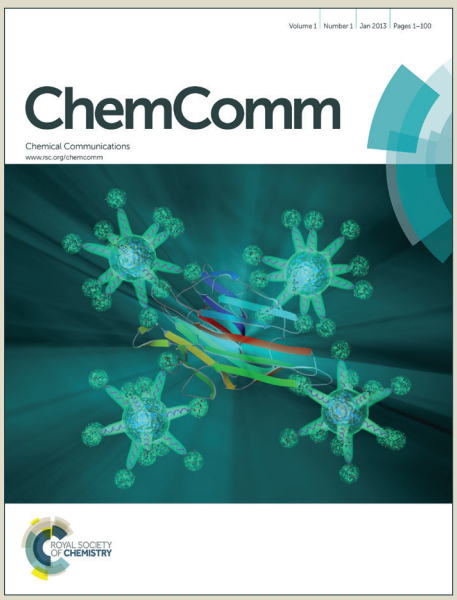

ROYAL SOCIETY OF CHEMISTRY

www.rsc.org/chemcomm

Journal Name

RSCPublishing

COMMUNICATION

One-pot Synthesis of Nitrogen and Sulfur Co-doped Graphene as Efficient Metal-free Electrocatalysts for Oxygen Reduction Reaction

Cite this: DOI: 10.1039/x0xx00000x

Received ooth January 2012,
Accepted ooth January 2012

DOI: 10.1039/x0xx00000x

www.rsc.org/

Xin Wang,[a] Jie Wang,[b] Deli Wang,[b] Shuo Dou,[a] Zhaoling Ma,[a] Jianghong Wu,[a] Li Tao,[a] Anli Shen,[a] Canbin Ouyang,[a] Qiuhong Liu[a] and Shuangyin Wang[a,c] *

A novel N, S co-doped graphene (NSG) was prepared by annealing graphene oxide with thiourea as the single N and S precursor. The NSG electrodes, as efficient metal-free electrocatalysts, show a direct four-electron reaction pathway, high onset potential, high current density and high stability for oxygen reduction reaction.

The oxygen reduction reaction (ORR) plays a key role in many fields, including fuel cells, metal-air batteries, corrosion, and biosensors.[1, 2] For low temperature fuel cells and metal-air batteries, the oxygen reduction reaction in the cathode is a major limited factor to obtain the expected performance. The ORR can occur either through a four-electron process or a less efficient two-step, two-electron process depending on the electrocatalysts utilized.[2] Nowadays, the typical electrocatalyst for ORR is the commercial Pt–based precious metal catalyst. However, Pt-based materials are extremely expensive and have only limited storage on the earth. Besides, Pt-based catalysts have shown sluggish ORR process, susceptibility to fuel crossover and poor stability. These disadvantages have tremendously limited the development and application of fuel cells and metal-air batteries. In this regard, numerous studies about metal-free or precious metal-free electrocatalysts have been conducted to find metal-free catalysts with excellent ORR performance. [1-3]

Of various metal-free electrocatalysts, nitrogen-doped carbon materials (including graphene, carbon nanotubes etc.) have been extensively investigated to replace Pt-based electrocatalysts for ORR. The improved performance of N-doped carbon for ORR originates from the charge transfer induced by the heteroatoms present in the graphitic framework to facilitate oxygen adsorption for ORR with relatively low overpotential, as proposed by Dai group.[1, 2] Recently, other elements besides N have been doped into carbon materials as metal-free electrocatalyst for ORR with improved performance compared to undoped carbon. [2-6] More recently, we have developed boron and nitrogen co-doped carbon nanotube (BCN nanotube)[2] and graphene (BCN graphene)[6] as efficient metal-free electrocatalysts for ORR. The synergetic effect between the two heteroatoms on the ORR activity has been investigated by the electrochemical characterizations and theoretical calculation. In our previous work, BCN graphene was prepared by annealing graphene oxide and boric acid mixture under flowing ammonia gas, which is toxic and dangerous to use.[6] Even though various heteroatoms co-doped carbon materials have been developed as metal-free catalyst for ORR, the development of new synthetic routes of this kind of novel materials is still in significant demand to improve the performance of metal-free catalysts for ORR.

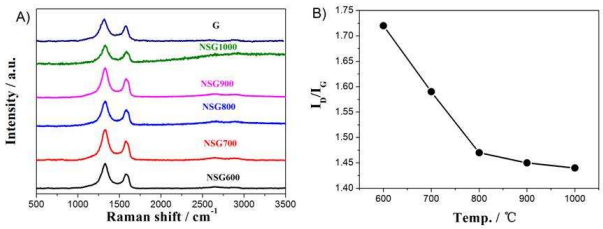

Figure 1. (A) Raman spectra of NSGs and undoped graphene; (B) the ID/IG ratio plotted against the annealing temperature.

In this work, we successfully developed a one-pot approach to prepare N and S co-doped graphene (NSG) by directly annealing graphene oxide (GO) and thiourea in argon, in which the single thiourea chemical was used as both N and S sources. It should be pointed out that thiourea could act as reducing agent to reduce graphene oxide as reported by Jayavel[7]. Therefore, during the temperature ramping from room temperature to the desired high temperature, GO was initially reduced by thiourea partially. Due to the solid phase nature and short reduction time, the reduction of graphene oxide is not complete. When the temperature is beyond 200 °C, thiourea decomposed to highly reactive N/S-rich species such as NH_3, H_2S, and CS_2, etc, and the reduction of graphene oxide by the thermal annealing became dominated. The removal of oxygen-containing groups of GO by the reduction generated defect sites,

which then reacted with N and S atoms decomposed from thiourea to complete the doping process.[8-10] The use of the single N and S precursor simplifies the synthetic process and makes it safe. Our physical characterizations indicate that the content of doped S increases and that of N decreases with the increase of the annealing temperature. The NSG samples we have obtained show improved ORR activity. This dual heteroatoms co-doped graphene was demonstrated to be a possible substitute for commercial Pt/C catalysts.

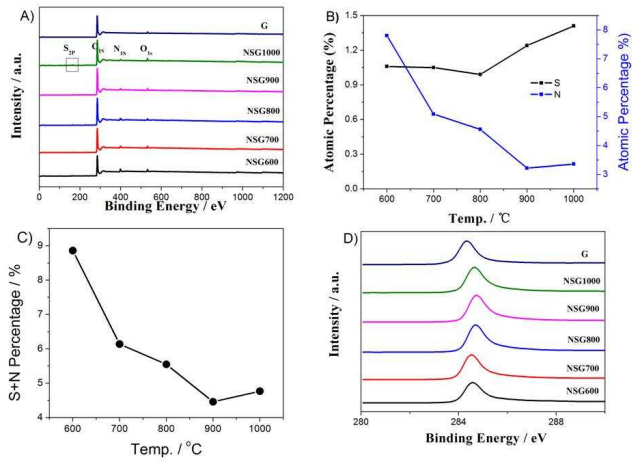

Figure 2. (A) The XPS survey spectra of NSGs and undoped graphene; (B) the S and N contents dependence on the annealing temperature; (C) the total S and N contents dependence on the annealing temperature; (D) the high-resolution C1s XPS spectra of NSGs and undoped graphene.

The NSGs were prepared by annealing graphene oxide in the presence of thiourea at various temperatures (see Supporting Information for experimental details). At the high annealing temperature, the decomposed N and S could be successfully incorporated into graphene. To investigate the structural morphology of the as-obtained N, S co-doped graphene (NSG), the scanning electron microscopy (SEM) image was collected for NSG700 (the value 700 stands for the annealing temperature, see Supplementary Information), as shown in Figure S1. It can be seen from Figure S1 that a large number of graphene-like nanosheets were observed, confirming that the doping process reserves the intrinsic morphology of graphene. The NSGs obtained at different temperatures were characterized by Raman to observe their further electronic properties. As can be seen from the Raman spectra (Figure 1A), the *D* band and *G* band were located around 1330 cm^{-1} and 1580 cm^{-1}, respectively. It has been found that the *G* band arises from the bond stretching of all sp^2-bonded pairs, including C-C, S-C, and N-C, while the *D* band is associated with the sp^3 defect sites.[6] The higher-order peak appeared at 2680 cm^{-1} and a small broad peak at 2910 cm^{-1} can be assigned to a combination of *D*+*D* and *D*+*G* bands. In the Raman spectra of carbon-based materials, I_D/I_G is an interesting indicator of the defects level. It can be seen from Figure 1A that all of the NSG samples show higher I_D/I_G ratio than undoped graphene (1.42) owing to the incorporation of defects by S- and N-doping. In the meantime, as the annealing temperature of the synthetic process increases, the I_D/I_G ratio of NSGs decreases from 1.72 to 1.44 (Figure 1B). On one hand, the decrease in the I_D/I_G ratio with the temperature increase may be due to the decrease of the total dopants (S+N) with the increase of the annealing temperature, as confirmed by the following X-ray photoelectron spectroscopy (XPS) results. On the other hand, it may also be due to the improved graphitic degree of the NSGs caused by the reduction effect and "self-repairing" of the graphene layer at the higher annealing temperature.[9]

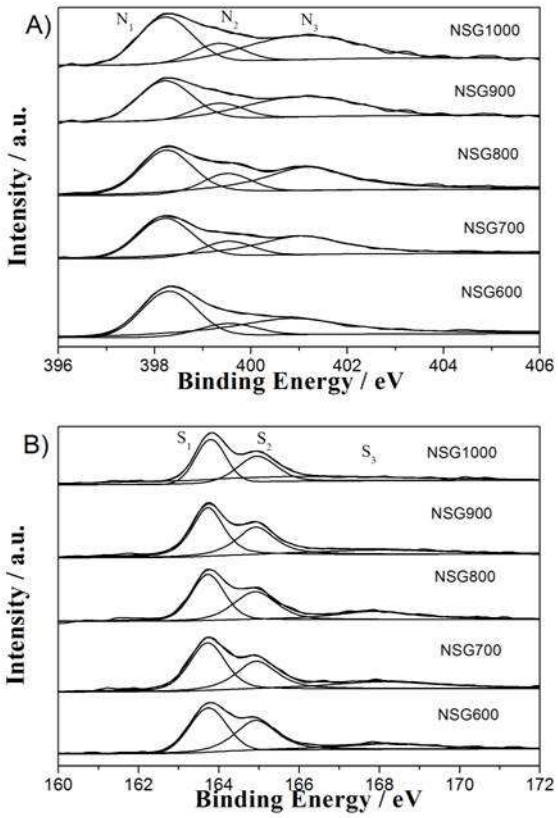

Figure 3. The high resolution N1s (A) and S2p (B) XPS spectra of NSGs annealed at different temperatures.

In order to confirm the composition of the as-obtained samples and the chemical states of the doped heteroatoms, XPS characterization was performed. As expected, all of the NSG samples show C, S, and N signals indicating the successful doping of S and N into graphene by annealing graphene oxide in the presence of thiourea (Figure 2A). The presence of an O 1s peak in the samples is probably attributed to the reason that the structure of reduced graphene is not fully recovered (see supporting information, Figure S2).[4] The XPS survey also gives the contents of N and S in the NSG samples, which are plotted against the annealing temperature (600~1000 °C), as shown in Figure 2B. It could be observed that the content of N in NSGs decreased with the increase of the annealing temperature, which is consistent with Dai's report on nitrogen doped graphene obtained by annealing graphene oxide in the presence of ammonia.[9] In contrast, the content of S increased with the increase of the annealing temperature, probably indicating the doping of S into graphene required higher temperature. And the overall doped content of S and N decreased with the

annealing temperature. The chemical state of C, N and S in NSGs was further studied by high resolution XPS. The high-resolution XPS C1s spectra given in Figure 2D clearly show an almost total loss of the oxygen component above 286 eV, while the carbon peak at 284.6 eV becomes more asymmetric and broadened due to N and S incorporation into the sp^2 network of graphene upon annealing with thiourea.[6,9]

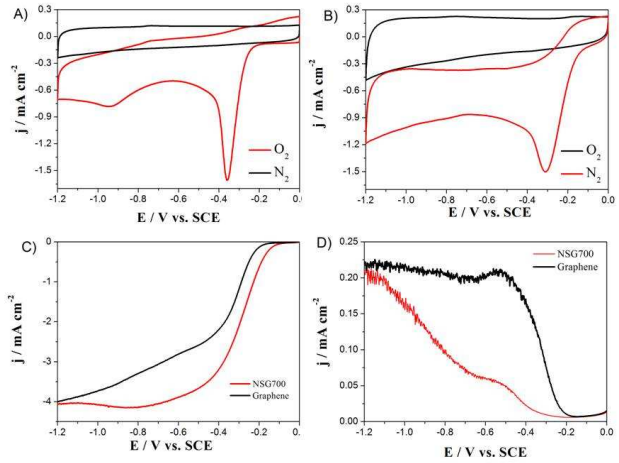

Figure 4. The cyclic voltammetry curves of oxygen reduction reactions on undoped graphene (A) and NSG700 (B) in nitrogen-(black) and oxygen-(red) saturated 0.1 M KOH electrolyte solution; the disc current density (C) and the ring current density (D) obtained from the LSV testing on electrode materials modified RRDE in oxygen-saturated 0.1 M KOH electrolyte.

We also investigated the bonding configurations of N and S atoms in the NSGs based on high-resolution N1s and S2p XPS spectra. The N1s peaks in the XPS spectra of NSGs annealed at 600 to 1000 °C were fitted into three peaks: pyridinic N (N_1), pyrolic N (N_2) and graphitic N (N_3) at the binding energies of around 398.2, 399.3, 401.2 eV, respectively[11] (Figure 3A) . The intensity of the high energy peaks (N_2 and N_3) increased with annealing temperature, indicating different N bonding configurations in graphene oxide reacted with thiourea at different temperatures.[9] The data suggested that higher temperature annealing of GO with thiourea afforded more graphitic N incorporated into the carbon network of graphene. Similarly, the high resolution S_{2p} peak can be fitted with three different peaks (Figure 3B). The major two peaks at the binding energies of 163.7 and 164.9 eV are in agreement with the reported $S_{2p3/2}$ (S_1) and $S_{2p1/2}$ (S_2) which are attributed to the binding sulfur in C-S bonds and conjugated –C=S– bonds, respectively.[12] The formation of the C-S may be due to the reaction between oxygen-containing groups in GO and H_2S/CS_2. Besides, the third sulfur peak (S_3) which results from oxidized sulfur (-SO_n-) at the binding energy of around 168.2 eV is detected in the XPS spectra.[12] From Figure 3B, it can be seen that S_3 decreases with annealing temperature, almost disappeared for NSG1000, indicating that oxidized sulfur could be transformed into sulfide groups at higher annealing temperatures.[12] The bond formation of –C-S-/-C=S- and C-N has been discussed in details in literatures.[8,9,13], Dai et al.[9] utilized ammonia for N doping of graphene and pointed out that the oxygen groups in graphene oxide were responsible for reactions with NH_3 and C-N bond formation. Xia et al. [13] used melamine as the N source to realize the N doping of graphene and suggested that the oxygen groups were reduced or removed at high temperature and the removal process of oxygen species provides active sites for nitrogen doping into graphene frameworks. Nitrogen atoms decomposed by N source can attack the active sites to complete the N doping. It is believed that S doping follows the similar mechanism.[8] The different bond types depends on the types of the active sites generated by oxygen removal at high temperature and can be converted at higher temperature as shown in Figure 3. In our work, thiourea was decomposed into NH_3, H_2S, and CS_2 etc. at high temperature, so the bond formation should follow the similar way in which N or S doping was realized with NH_3, H_2S, and CS_2.

To investigate the electrocatalytic activity of NSGs, the ORR behavior on the electrodes was measured in 0.1 M KOH solution using a conventional three-electrode system. As shown by the cyclic voltammogram (CV) curves in Figure 4A-B, both undoped graphene and NSG700 showed a substantial reduction process in the presence of oxygen, whereas no obvious response was observed under nitrogen. The onset and peak potentials of ORR on NSG700 are more positive, and the current densities much higher, than those on undoped graphene, indicating the advanced role of doped heteroatoms to enhance ORR activity, consistent with our previous work on BCN graphene.

To investigate the kinetics of ORR on NSGs, rotating ring disc electrode (RRDE) voltammetry (linear sweep voltammetry, LSV) was performed at the rotation rate of 1600 rpm in O_2-saturated 0.1 M KOH solution with a scanning rate of 10 mV s^{-1}. As shown in Figure 4C, the typical two-step pathway was observed for undoped graphene, indicating a successive two-electron reaction pathway, instead of the direct four-electron pathway, consistent with literature reports.[6] On the NSG700 electrode, the LSV curves show a single-step wide platform, indicating a four-electron ORR process. Interestingly, the onset potential (*i.e.,* the potential at which the ORR starts to occur) for ORR on undoped graphene is much more negative than that of NSG700. And also, NSG700 shows more positive onset potential than most of reported metal-free electrocatalysts, as shown in Table S1. Besides, the current density of ORR on undoped graphene electrode is also much lower than that NSG700. In Figure 4D, based on the RRDE testing, we also obtained ring current, reflecting the oxidation of the ORR by-products on the electrode.[2,6] It could be observed that the ring current on undoped graphene is much higher than that on NSG700, indicating more intermediate by-products of ORR were produced on undoped graphene. With the tested disc and ring currents, we could calculate the electron transfer number (*n*) of ORR according to the following equation:

$$n = \frac{4 j_D}{j_D + \frac{j_R}{N}}$$

In this equation, j_D is the faradic disc current, j_R is the faradic ring current (Figure 4D), and *N* is the collection efficiency (0.37) of the ring electrode. Based on the calculation, the electron transfer number of ORR on NSG700 is 3.91 at -0.5V, which is closer to the theoretical 4e reaction pathway than N or S doped graphene in Yang's report.[12]

Therefore, on the NSG700 electrode, ORR follows a direct 4e pathway by directly forming OH^- ions as the final product, as is the case with the commercial Pt/C electrode. This confirmed that N,S co-doped graphene is more likely to be a substitution for Pt/C than N or S doped graphene which is consistent with Qiao's report.[4] Therefore, the as-prepared NSGs show significantly improved ORR activity in terms of electron transfer number, onset potential and current density. We also investigated the dependence of ORR activity of NSGs on the annealing temperatures, as demonstrated by the LSV curves in Figure S3. It could be observed that, of the NSG electrodes obtained at different annealing temperatures, the NSG700 is the most active in terms of the onset potential probably due to the optimized composition and heteroatom bonding configurations of NSG at this annealing temperature (700 °C).

Finally, the stability of the as-prepared NSG700 electrocatalysts was also examined compared with the commercial Pt/C catalysts, as shown in Figure S4. We performed accelerated CV scanning for 2000 cycles at a scan rate of 100 mV s^{-1} within the potential window of -0.5 V to 0V. Figure S4 shows the LSV curves of NSG700 and Pt/C before and after the accelerated CV scanning of 2000 cycles. As can be seen, after continuous CV scanning of 2000 cycles, the onset potential of ORR on Pt/C electrocatalyst shifted negatively by 45 mV, while the onset potential of ORR on NSG700 became even more positive probably due to the further activation by the continuous CV scanning. The results clearly indicate that the electrochemical activity of NSGs is much more stable than that of the commercial Pt/C.

In summary, we have successfully fabricated a novel N, S co-doped graphene through a simple but efficient and versatile annealing approach with thiourea as the single N and S precursor. The as-prepared NSG electrodes show a direct 4e reaction pathway, and high onset potential, high current density and high stability for ORR in the alkaline medium. The as-obtained materials show potential to be used as efficient metal-free ORR electrocatalysts for fuel cells, metal-air batteries, and even other energy conversion and storage devices.

This work was supported by Marie Curie International Incoming Fellowship Programme of European Commission and Youth 1000 Talent Programme of China.

Notes and references

[a] State Key Laboratory of Chem/Bio-Sensing and Chemometrics, College of Chemistry and Chemical Engineering, Hunan University, Changsha, 410082, P. R. China.
Email: shuangyinwang@hnu.edu.cn
[b] College of Chemistry and Chemical Engineering, Huazhong University of Science and Technology, Wuhan, 430074, P. R. China.
[c] School of Physics and Astronomy, The University of Manchester, Great Manchester, M13 9PL, United Kingdom.

† Electronic Supplementary Information (ESI) available: Experimental details and supplementary information available. See DOI: 10.1039/c000000x/

1. K. Gong, F. Du, Z. Xia, M. Durstock and L. Dai, *Science*, 2009, 323, 760-764.
2. S. Wang, E. Iyyamperumal, A. Roy, Y. Xue, D. Yu and L. Dai, *Angewandte Chemie International Edition*, 2011, 50, 11756-11760.
3. Z. Liu, H. Nie, Z. Yang, J. Zhang, Z. Jin, Y. Lu, Z. Xiao and S. Huang, *Nanoscale*, 2013, 5, 3283-3288.
4. J. Liang, Y. Jiao, M. Jaroniec and S. Z. Qiao, *Angewandte Chemie International Edition*, 2012, 51, 11496-11500.
5. Z. Yang, Z. Yao, G. Li, G. Fang, H. Nie, Z. Liu, X. Zhou, X. A. Chen and S. Huang, *ACS nano*, 2011, 6, 205-211.
6. S. Wang, L. Zhang, Z. Xia, A. Roy, D. W. Chang, J. B. Baek and L. Dai, *Angewandte Chemie International Edition*, 2012, 51, 4209-4212.
7. K. Satheesh, R. Jayavel, *Materials Letters*, 2013, 113, 5-8.
8. H. L. Poh, P. Simek, Z. k. Sofer and M. Pumera, *ACS nano*, 2013, 7, 5262-5272.
9. X. Li, H. Wang, J. T. Robinson, H. Sanchez, G. Diankov and H. Dai, *Journal of the American Chemical Society*, 2009, 131, 15939-15944.
10. Y. Su, Y. Zhang, X. Zhuang, S. Li, D. Wu, F. Zhang and X. Feng, *Carbon*, 2013.
11. Y. Wang, Y. Shao, D. W. Matson, J. Li and Y. Lin, *Acs Nano*, 2010, 4, 1790-1798.
12. S. Yang, L. Zhi, K. Tang, X. Feng, J. Maier and K. Müllen, *Advanced Functional Materials*, 2012, 22, 3634-3640.
13. Z. Sheng, L. Shao, J. Chen, W. Bao, F. Wang, X. Xia, , *ACS Nano*, 2011, 5, 4350-4358.

